A morphodynamic stability analysis of gravel beach cross-section by 1D numerical model

Authors:

¹Assoc.Prof. **Goran Lončar**
goran.loncar@grad.hr

¹Assist.Prof. **Dalibor Carević**
car@grad.hr

¹Assist.Prof. **Damir Bekić**
damir.bekic@grad.hr

¹**Maria Babić**, BSc. CE
maria.babic@student.grad.hr

¹**Nina Grbić**, BSc. CE
nina.grbic@student.grad.hr

¹**Vjera Pranjić**, BSc. CE
vjera.pranjic@student.grad.hr

¹University in Zagreb
 Faculty of Civil Engineering
 Department for Water Research

Subject review

Goran Lončar, Dalibor Carević, Damir Bekić, Maria Babić, Nina Grbić, Vjera Pranjić

A morphodynamic stability analysis of gravel beach cross-section by 1D numerical model

A stability analysis of gravel beaches, and development of their cross-sectional profiles under the action of gravitational wind waves, is described in the paper. The analysis was conducted using the numerical modelling technique. The modelling approach was also applied in the analysis of wave deformations and morphodynamics on the example of a gravel beach in Medveja. The designed beach cross-sections correlate well with the measured Medveja beach cross-sections, and so the methodology and the beach material erosion estimate can be applied in practice when making decisions at various design stages.

Key words:

numerical model, gravel beach, wind waves, beach material erosion

Pregledni rad

Goran Lončar, Dalibor Carević, Damir Bekić, Maria Babić, Nina Grbić, Vjera Pranjić

Analiza morfodinamičke stabilnosti poprečnog profila šljunčane plaže

U radu je opisna analiza stabilnosti šljunčanih plaža i razvoj njihovog profila u poprečnom smjeru pri djelovanju gravitacijskih vjetrovnih valova. Analiza je provedena tehnikom numeričkog modeliranja. Modelski pristup primijenjen je i u analizi valnih deformacija i morfodinamike na primjeru šljunčane plaže Medveja. Rezultantni modelski profili plaže koreliraju s izmjerenim poprečnim profilima plaže Medveja, pa se metodologija i dobivena procjena erozije materijala plaže mogu praktično primijeniti pri donošenju odluka u raznim fazama projektiranja.

Ključne riječi:

numerički model, šljunčana plaža, vjetrovni valovi, erozija materijala plaže

Übersichtsarbeit

Goran Lončar, Dalibor Carević, Damir Bekić, Maria Babić, Nina Grbić, Vjera Pranjić

Analyse der morphodynamischen Stabilität des Querschnittsprofils von Kiesstränden

In dieser Arbeit werden Stabilitätsanalysen von Kiesstränden und die Entstehung ihrer Querschnittsprofile unter Einwirkung durch Wind entstehender Gravitationswellen beschrieben. Die Analyse wurde mittels numerischer Modellierung durchgeführt. Dieser Modellansatz wurde auch bei der Analyse der Wellendeformationen und des morphodynamischen Verhaltens am Beispiel der Querschnittsprofile des Strandes Medveja angewandt. Die resultierenden Modellprofile des Strandes Medveja korrelieren mit den aus Messungen ermittelten Querschnittsprofilen. Somit können die Methodologie und die resultierende Bewertung der Strandmaterialerosion bei Entscheidungen in verschiedenen Planungsphasen praktisch angewandt werden.

Schlüsselwörter:

numerisches Modell, Kiesstrand, Windwellen, Erosion von Strandmaterial

1. Introduction

Beaches are assets of significant environmental and economic value and are frequently used for recreation and accommodation purposes. An increasing trend of extending available beach capacities has been noted over the past two decades. For a rational response to this challenge, a hydrodynamically favourable position should be chosen, and a satisfactory reclamation material should be selected. Poor choices will lead to material loss (movement of sediments into a deeper sea layer) and degradation of the landscape and sea-bed biodiversity. The gravel beach category implies a considerable content of gravel in the mixture and, according to the standardised Udden-Wentworth classification, the grain diameter should vary from 2 to 64 mm.

Development of novel technologies such as those involving optical measuring devices, and the application of a new generation of cameras and acoustic devices, have opened the possibility of developing laboratory and in-situ investigations focusing on beach development under various environmental conditions. Concurrently, new models of gravel beach morphodynamics have been established [1]. Previous studies mainly concentrated on the long-term morphological changes of beach profile [2-4], while comprehensive analyses of short-term changes have recently become a topical research issue [5-7].

An interaction between the waves and beach in coastal zones is a complex process, especially if the cross-sectional beach profile is mainly composed of gravel [8]. Over the course of time, the morphological action becomes evident as the initial beach profile of constant slope changes (anthropogenic impact) as a consequence of erosion and sedimentation alterations. The erosive activity (material loss) is primarily concentrated in the swash zone and its intensity depends on the frequency of incidental wave spectra during the period of analysis [9]. The eroded material is moved to a greater depth where it is deposited, and as such it represents a "loss-expense" of reclamation material for the beach. In cases of naturally balanced cross-sectional beach profiles, such excessive wave load conditions are followed by a period of moderate wave climate, during which the previously deposited material is once again drawn upwards to the beach face. This alternation of loss and gain of beach material is typical for beaches characterized by natural balance of longitudinal profile. An equilibrium longitudinal profile of the wet part of beaches is described by empirical formulae [10-12] in which the relationship between the depth and the distance from coast is approximately defined.

Empirical formulae of equilibrium longitudinal profiles [10-12] rely on a single input data: grain diameter of beach material. A comparison of gravel beach profiles calculated by such terms with the profiles measured in nature point to a low reliability of empirical terms formulae [13-15], except in the case of pronouncedly homogenous environmental conditions and high costs of investigation works [16]. Moreover, the empirical terms define the equilibrium cross-sectional profile in exponential form, which is certainly complex enough to construct. According to our knowledge, there are still no publications and/or studies that would systematically describe the relationship between the intensity of morphological change (erosion and sedimentation across the beach profile) and environmental-external conditions (wave climate). Consequently, designers experience difficulties when having to decide on the appropriate grain size of filling material and the slope of beach profile, and are unable to provide reliable and fast cost estimates for variants of planned projects.

This paper presents numerical modelling results of morphological changes of gravel beach profiles in a range of present-day environmental conditions. Final results are presented in form of charts enabling a simple estimate of the quantity of eroded beach material as dependent on the prevailing wave conditions, initial beach slope, and grain size of filling material.

The following relevant parameters are included in the research: diameter of beach grain material d_{50} = 10, 20, 30 mm, deep-water significant wave height H_S = 0.7, 1, 1.5, 2 m, wave steepness I_W = 1:12, 1:15, 1:20, 1:25, and initial beach slope I_B = 1:4, 1:6, 1:8, 1:10. JONSWAP wave spectra are used in each analysis with the parametrisation of g = 3.3. The results of morphological changes are presented for the case of continuous wave action during 3 hours and during 12 hours.

In addition to the previously mentioned parametric analysis, the morphological model analyses were also conducted for the cross-sectional profile of Medveja Beach subjected to the real-wave actions. The numerical model was validated based on comparison with the measured beach profiles of Medveja Beach.

It should be noted that the following two processes simultaneously occur during wave action at a gravel beach: erosion of material toward a greater depth, and gain of beach material at the beach. These processes occur in the wave direction, i.e. in the direction of incidental waves, and in the opposite direction. Thus a two-dimensional movement of beach material occurs (along and across the beach). The beach degradation processes usually occur at a certain angle with respect to the beach and, in case of a typical beach in Croatia, the wave action is usually not perpendicular to the beach transverse line. This paper presents a beach-material stability analysis for a single cross-section of the beach, which is in line with the incidental wave direction. Therefore, the analysis presents only a cross-sectional component of the beach material movement, while disregarding the longitudinal movement component generated by inclined direction of incidental waves.

2. Numerical model

If a dominant physical process is recognised and introduced into the process-oriented numerical model, then it can be applied on a global level. Therefore, numerical models represent an improvement when compared to empirical models. A considerable attention has recently been given to the development of models that analyse wave dynamics on sandy beaches [17, 18] (grain diameter ranging from 0.06 mm to 2 mm). On the other hand, relatively fewer models have been developed for the analysis of beach morphodynamics with mixed material, or mostly gravel material [19-21]. The reason for this are relatively limited

datasets of measurements in nature and in laboratory conditions, which are insufficient for proper validation of model parameters and results.

The "open-source" model XBeach-G was used in this study (http://oss.deltares.nl). It resolves the morphodynamics of cross-sectional gravel beach profiles subjected to wind wave action in transitional and shallow-water areas. The processes of seawater infiltration and exfiltration in and out of the gravel beach body during the wave rise along the beach face are included using newly developed models of the interaction of surface and subsurface flows [22]. This interactive process is of much greater significance in the case of gravel beaches compared to sandy beaches [23]. The interactive surface and subsurface flow processes are calculated in the model through a single vertical layer. Although equations are averaged for the vertical layer, two quasi 3D models are used in parallel for the calculation of vertical distribution of velocity and pressure on the surface and on the bottom of the water column (non-hydrostatic approximation of pressure distribution). A detailed description of basic equations used by the numerical model is provided in paper [23].

Surface flow was resolved using the predictor-corrector numerical scheme [24]. This scheme has a characteristic second order accuracy in the smooth resolution zone and the first order accuracy in the area of discontinuity [25]. The scheme is conservative on the issue of mass and momentum conservation [26], which enables accurate presentation of the drying and flooding of numerical nodes and the critical and supercritical flow. Subsurface pressure is resolved with the first order central differentials. Momentum calculation in horizontal direction in the spatial scale less than grid spatial increment relies on the Smagorinsky model of horizontal viscosity [27]. The Keller-Box method was used for the calculation of pressure gradient in vertical direction [28]. Subsurface flow in horizontal direction was treated according to the Darcy's law, with additional customisation for the turbulent flow regimen [29]. In order to calculate non-hydrostatic distribution of pressures in subsurface flow, the piezometric level was approximated with a parabola in vertical direction with the bottom boundary condition expressed with vertical velocity 0, imposed for the level of free water surface and constant velocity gradient along the vertical [15]. The inflow and outflow occur where the surface and sub-surface waters are not in contact [30]. Therefore, the infiltration occurs at the location where the surface flow submerges the area with the groundwater level lower than the beach level, and the percolation of surface water into the subsurface layer is dependent on the pressure gradient along the wetted front [20].

The numerical model used (Xbeach-G) was validated on the basis of a small-scale research on physical model [21] and a detailed in-situ research, and using data obtained by long-range detection for several gravel beaches along the English coastline [7].

The following values were used in numerical model analyses: significant wave height H_s = 0.7; 1; 1.5; 2 m, with the related peak wave periods T_p with which desired wave steepness values were obtained: 1:12, 1:15, 1:20, 1:25 (Table 1). Wave lengths were defined for deep-water conditions L_s = gT_s^2/(2·p), where the ratio between significant and peak wave periods was defined with the relation T_s = T_p = T_s ·1.05 [31]. JONSWAP wave spectra were used with parametrisation g = 3.3. The values presented in [32] were adopted in the parametrisation of the underground flow model for the coefficient of permeability k. These values were related to the beach material grain diameter (d_{50} = 10 mm → k = 0.15 m/s, d_{50} = 20 mm → k = 0.65 m/s, d_{50} = 30 mm → k = 1.8 m/s,). The following values were adopted in the morphodynamic module: Shield's dimensionless sediment friction coefficient: 0.025, phase shift in Nielsen's boundary layer: 25⁰, angle of repose: 35⁰.
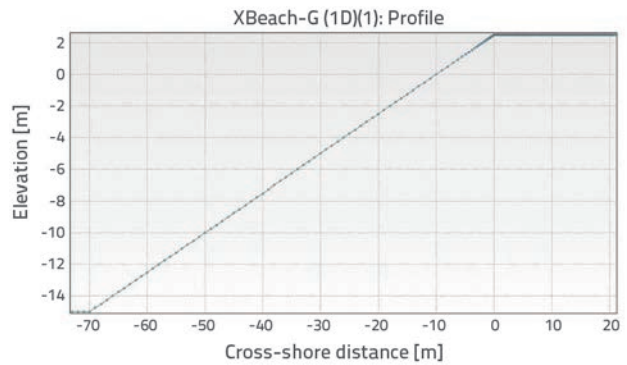

Figure 1. Discretisation of 1D numerical model with variable step between calculated nodes (initial beach slope 1:4)

Table 1. Analysed significant wave heights H_s and accompanying peak wave periods T_p with which desired wave steepness values were obtained I_w 1:12, 1:15, 1:20, 1:25

	wave steepness values					wave steepness values			
	1:12	1:15	1:20	1:25		1:12	1:15	1:20	1:25
H_s	deep water L_s [m]				H_s	deep water T_p = T_s*1.05 [s]			
0.7	8.4	10.5	14	17.5	0.7	2.4	2.7	3.1	3.5
1	12	15	20	25	1	2.9	3.3	3.8	4.2
1.5	18	22.5	30	37.5	1.5	3.6	4.0	4.6	5.1
2	24	30	40	50	2	4.1	4.6	5.3	5.9

3. Empirical model

The empirical model of the equilibrium longitudinal bottom profile is presented in papers [10, 11] and it refers only to sediment diameter d_{50} in the simple analytical form $h(y)$ = $A(d)$ $y^{2/3}$, where y is the horizontal distance in longitudinal direction at calm sea level and $A(d)$ is the empirical parameter defined with the relation $A(d)$ = 0,067$d_{50}^{0,44}$. The equilibrium profile for the sediment granulation d_{50} = 10, 20, and 30mm, is shown in Figure 2.

For the estimation of 'erosion-damaged' gravel beach surfaces (material lost to depths) following wave action, Van de Meer proposes an empirical model defined with equation (1) [12]:

Table 2. Values of eroded surface *A* according to empirical model [12] for analysis of range of significant wave heights, wave steepness values, beach and bottom slope with adopted parameter values $\rho_{\check{s}}$, ρ_M, *N*, *P* and d_{50} = 10 mm

	l_W = 1:12 ; d_{50} = 10 mm															
H_S [m]	0.7	1	1.5	2	0.7	1	1.5	2	0.7	1	1.5	2	0.7	1	1.5	2
l_B	1:4	1:4	1:4	1:4	1:6	1:6	1:6	1:6	1:8	1:8	1:8	1:8	1:10	1:10	1:10	1:10
A [m²]	5.6	33.3	253	1066	2.0	11.7	89.1	375	1.0	5.7	43.0	181	0.5	3.2	24.5	103
	l_W = 1:15 ; d_{50} = 10 mm															
H_S [m]	0.7	1	1.5	2	0.7	1	1.5	2	0.7	1	1.5	2	0.7	1	1.5	2
l_B	1:4	1:4	1:4	1:4	1:6	1:6	1:6	1:6	1:8	1:8	1:8	1:8	1:10	1:10	1:10	1:10
A [m²]	7.4	44.0	334	1409	2.6	15.5	117	496	1.3	7.5	56.8	239	0.7	4.3	32.4	136
	l_W = 1:20 ; d_{50} = 10 mm															
H_S [m]	0.7	1	1.5	2	0.7	1	1.5	2	0.7	1	1.5	2	0.7	1	1.5	2
l_B	1:4	1:4	1:4	1:4	1:6	1:6	1:6	1:6	1:8	1:8	1:8	1:8	1:10	1:10	1:10	1:10
A [m²]	10.6	63.1	479	2018	3.7	22.2	168	711	1.8	10.7	81.4	343	1.0	6.1	46.4	195
	l_W = 1:25 ; d_{50} = 10 mm															
H_S [m]	0.7	1	1.5	2	0.7	1	1.5	2	0.7	1	1.5	2	0.7	1	1.5	2
l_B	1:4	1:4	1:4	1:4	1:6	1:6	1:6	1:6	1:8	1:8	1:8	1:8	1:10	1:10	1:10	1:10
A [m²]	14.0	83.4	633	2668	4.9	29.4	223	940	2.4	14.2	107	453	1.4	8.1	61.3	258

$$A = \frac{H_S^5}{9161,3 \, \Delta^5 d^3 P^{0,9} N^{-0,5} \xi^{-2,5}} \tag{1}$$

where is:

A - the eroded surface across the profile
H_S - the significant wave height
d - the grain change
$\rho_{\check{s}}$ - he gravel grain density (adopted as 2600 kg/m³)
ρ_M - the seawater density (adopted as 1028 kg/m³)
Δ - the relative density = $(\rho_{\check{s}}/\rho_M)$ - 1
N - the number of waves (adopted as 7500)
P - the notational permeability (adopted as 30 %)
ξ - Iribarren number, $\xi = \tan\alpha/s^{0,5}$
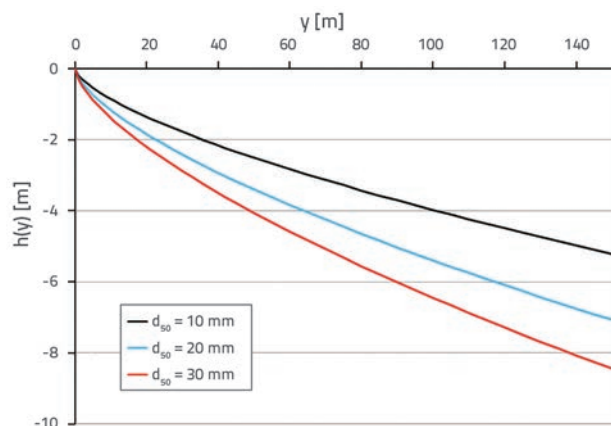   (tanα - beach slope, s - wave steepness, s = H_s / L_s)

Figure 2. Equilibrium longitudinal bottom profile for sediment granulation according to empirical terms d_{50} = 10, 20, and 30 mm, presented in [10, 11]

In Table 2, eroded surface (*A*) values are shown for analysis of the range of significant wave heights, wave steepness values, bottom and beach slope, with the previously adopted parameter values $\rho_{\check{s}}$, ρ_M, *N*, *P* and d_{50} = 10 mm. The presented empirical models [10-12] were also used in the following sections for comparison with the numerical model results.

4. Intensity of erosion in a wide range of environmental conditions

Relationships between the volume of beach material lost in the depths (erosion, economically speaking — expense) and the input data H_s, l_B, l_W, d_{50} for the numerical model XBeach-G, are given in Figures 3 and 4. The eroded volume refers to one meter of beach width (multiplication of eroded area by one meter of beach width). Figure 3 consolidates every numerical calculation result and shows three polynomial interpolations that can be used to directly calculate the eroded surface, or volume. It should be mentioned that the results obtained by polynomial interpolations have an average error (AE) of +0.15 m (*d* = 10 mm), +0.05 m (*d* = 20 mm) and +0.01 m (*d* = 30 mm), and the root mean square error (RMSE) of 2.0 (*d* = 10 mm), 1.61 (*d* = 20 mm) and 1.24 (*d* = 30 mm), related to the values calculated via the numerical model. A detailed view of the eroded area as a function of input parameters H_s, l_B, l_W, d_{50}, more appropriate for the necessary practical applications, is given in Figure 4.

Compared to results shown in Table 2, the obtained values are by one order lower than the estimated volumes of erosion obtained with the empirical formula (1). Here, the increase in wave steepness and height values contributes to the increase in differences. This difference need not be surprising given that formula (1) is obtained on the basis of erosion measurements

primarily from the armour layer of the breakwater structure in the physical model and in nature, where the grain diameters are by one to two orders greater in size compared to the diameter of the beach gravel material.
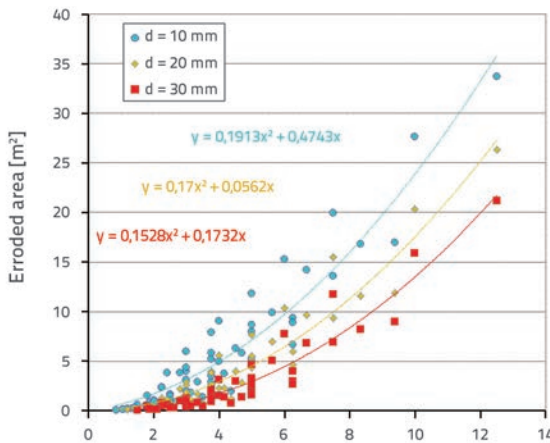

Figure 3. Calculated volumes (area * 1m' of beach) of eroded beach material as a function of input calculation parameters H_s, I_B, I_W, d_{50} (model XBeach-G), with interpolation polynomials
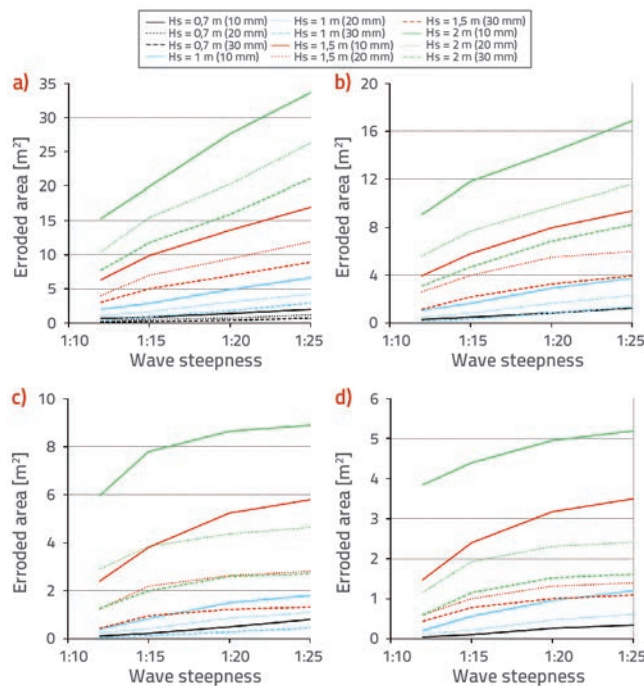

Figure 4. Volume (surfaces x 1m' of beach) of eroded beach material dependent on input parameters H_s, I_B, I_W, d_{50} from numerical model XBeach-G: a) I_B = 4; b) I_B = 6; c) I_B = 8; d) I_B = 10

5. Estimation in real conditions (case study: Medveja Beach)

The survey plan of the entire Medveja Bay was developed on the basis of measurements conducted on 23/12/2013 (Figure 5). Figure 5 also shows the beach material sampling position

on 10/05/2015. It was established by laboratory testing of material grading that d_{50} = 14.5 mm (50 % of the grading curve of the tested sample).

An appropriate information about the perceived general dynamics of beach material was gained based on field survey and discussions with professionals in charge of beach maintenance. The central and southern parts of the beach (Figure 5, green line) were perceived to be more exposed to long-shore material transport as a result of severe wave action, while the beach "recovered" under conditions of moderate wave action from incidental directions ranging from ENE-SSE. On the other hand, the northern part of the beach (Figure 5, pink line) showed a more significant propensity for cross-shore transport, and that only in conditions of waves generated by southern winds. A more noticeable change can be observed along the analysed profile during strong storms and more pronounced wave action from a southerly direction (Figure 5).

It can also be seen that the most intensive erosion occurs in the mean sea level zone. If the calm wave climate period between two storms is long enough, the cross-shore profile returns to its original form. From this it can be assumed that the beach profile measured on 23/12/2013 (Figure 5) represents the characteristic situation after a long period of mild wave climate, i.e. after a long absence of intensive wave action from the southern incidental direction.
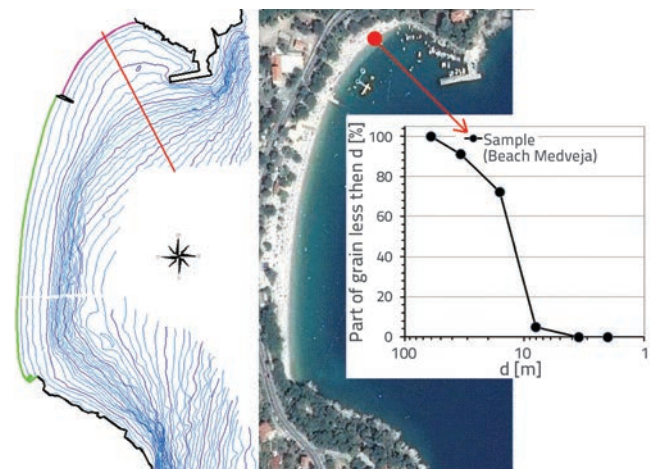

Figure 5. Bathymetry of the Medveja Beach aquatorium (depth step 1 m), position of sampling material and grain size distribution results

In the previous period, large flush flows maintained natural supply of larger quantities of gravel material into the Medveja Beach. Due to development of the area that supply of gravel decreased significantly. The beach sediments are of different sizes as the sediments spread according to the wave action strength (Figure 6, condition in November 2010). Figure 6 also shows the condition at Medveja Beach in February 2011 after several storm surges. The erosion of material into a deeper sea zone is clearly visible. The restoration and profiling of the beach was performed by supply of larger quantities of gravel.
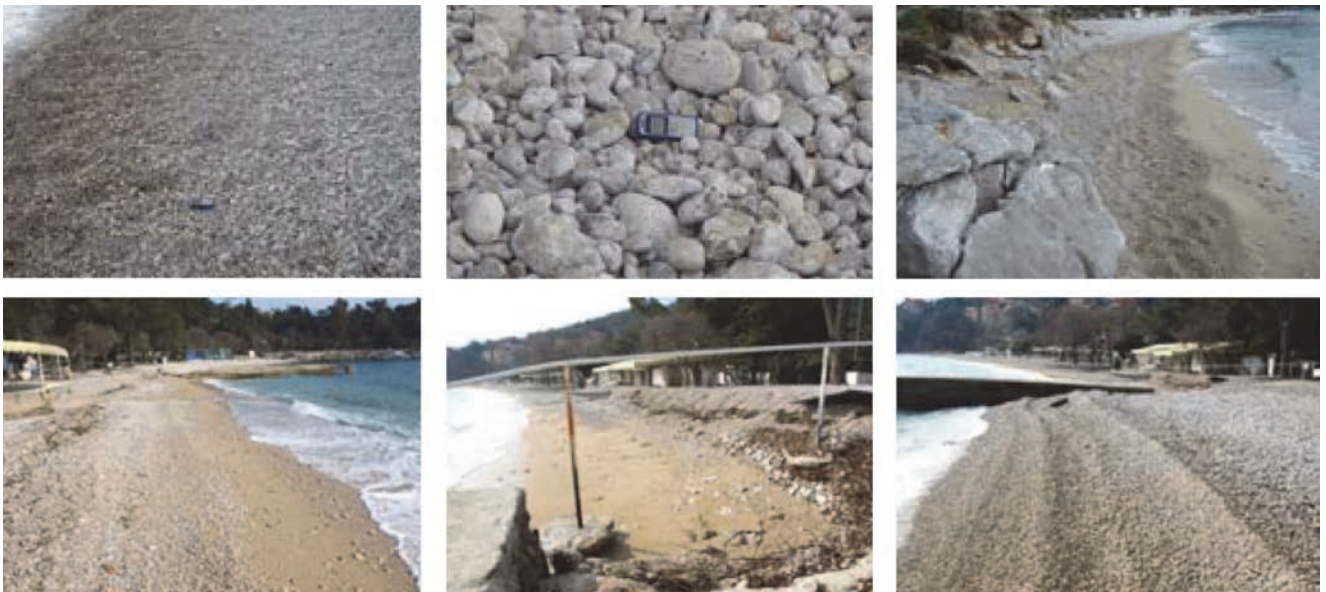
Figure 6. Different sizes of gravel as the sediments are spread according to the wave action strength (top, November 2010) and condition in February 2011, after several storm surges (bottom)

In order to check (possible) practical implications of the results from the previous part of this section, an analysis with several numerical modelling steps-phases was conducted, as shown below. Originally, the numerical model was established for wave generation and wave deformation for the entire Adriatic basin (Figure 6, regional model), resulting in a space-time distribution of the significant wave height H_s and peak period T_p. From the overall simulation period (2013), the situations with exceeded thresholds were selected $H_s > 0.2$ m, $T_p > 2.7$ s in a range of incidental directions ESE (112,5⁰) – S (180⁰) at the entrance to Medveja Bay. Because of the insufficiently detailed numerical grid used in the regional model to solve all relevant wave deformation processes (shallowing, refraction, diffraction) in Medveja Bay, another model with a finer-resolution spatial scale was established (Figure 6, local model). Each isolated situation was further analysed in the local model, with boundary conditions (H_s, T_p, incidental wave action) acquired from the regional model results. In addition, wave deformations calculated with the local model were followed to the starting point of the profile at isobath -10 m (Figure 5), giving input information (boundary conditions) for the numerical model of morphological change along the analysed profile.

Finally, numerical calculations of erosion along the analysed profile (Figure 5) in "real" dynamic conditions of intensive wave action (unsteady boundary conditions H_s, T_p) were made, including comparison with the results given in the diagram of erosion for a wide range of environmental conditions (Figure 4).

5.1. Regional and local model of wave generation and deformation

The area included in the spatial domain of the numerical wave generation and wave deformation model (regional and local

models) is shown in Figure 7. This figure also shows the applied discretisation model with finite volumes. The distance between numerical nodes is variable and ranges from 8000 (12) m in the deep-water area to 250 (2) m in the coastline area. The values given in parentheses are related to the local model calculation grid. The spatial domain of the regional model comprised the entire Adriatic Sea, and the wave data recordings for validation of the numerical wave generation model were available from the open sea location. However, is should be noted that Medveja Beach is dominantly influenced by the action of waves generated in a relatively closed maritime zone, and by the winds exhibiting local characteristics.

The spectral numerical model Mike 21/SW (www.dhigroup.com) was used for the numerical analysis. This model simulates generation, deformation and attenuation of gravitational wind waves in the open-sea and coastal areas. The spectral formulation based on the work of Komen et al [33] was used. A logarithmic scale with a minimum frequency of 0.08 Hz (wave period 12.5 s) and a maximum frequency of 0.95 Hz (wave period 1.05 s), featuring 28 discrete steps, was used for the spectral discretisation in the frequency domain. The model included processes of wave generation with wind, wave nonlinear interaction, refraction, diffraction and shoaling, as well as the dissipative process caused by bottom friction, surface white-capping, and wave breaking. The multi-sequential Euler explicit method was used for the propagation of wave action. The source function in the wave action conservation equation was treated on the basis of the 3rd generation, and numeric integration was conducted according to the methodology described in the work of Hercbach and Jansen [34]. The connective flux was calculated with an 'upwind' numerical scheme of the first order.

Initial conditions in the regional model (01/01/2008 to 01/01/2013 0:00) were defined with the zero wave spectrum,

i.e. with the absence of initial wave movement in the modelled area. In the period under study (01/01/2008 to 15/11/2013, and 01/01/2013 to 01/01/2014), the regional model was forced with wind fields from the atmospheric model Aladin-HR with the 8 km spatial resolution and the 3-hour time resolution [35, 36].

Several sources were used for calibration of the regional model. The first source were measurements from the wave recording station situated in the northern Adriatic open-sea area (Ivana Platform; φ = 44°44,5' N, λ = 13°10,2' E). The comparison of measured and modelled significant wave heights at the wave recording station over the period from 01/01/2008 to 15/11/2008, and histogram errors (measured H_s and modelled H_s) for the same period, are shown in Figure 8. Statistical errors of modelled values for half-hourly average wave heights at the wave recording station in relation to measured values for the simulation period from 01/01/2008 to 15/11/2008 have the following feature(s): average error AE = 0.064, and the root mean square error PMSE = 0.0038. The second source are the measured wave data from the breakwater position
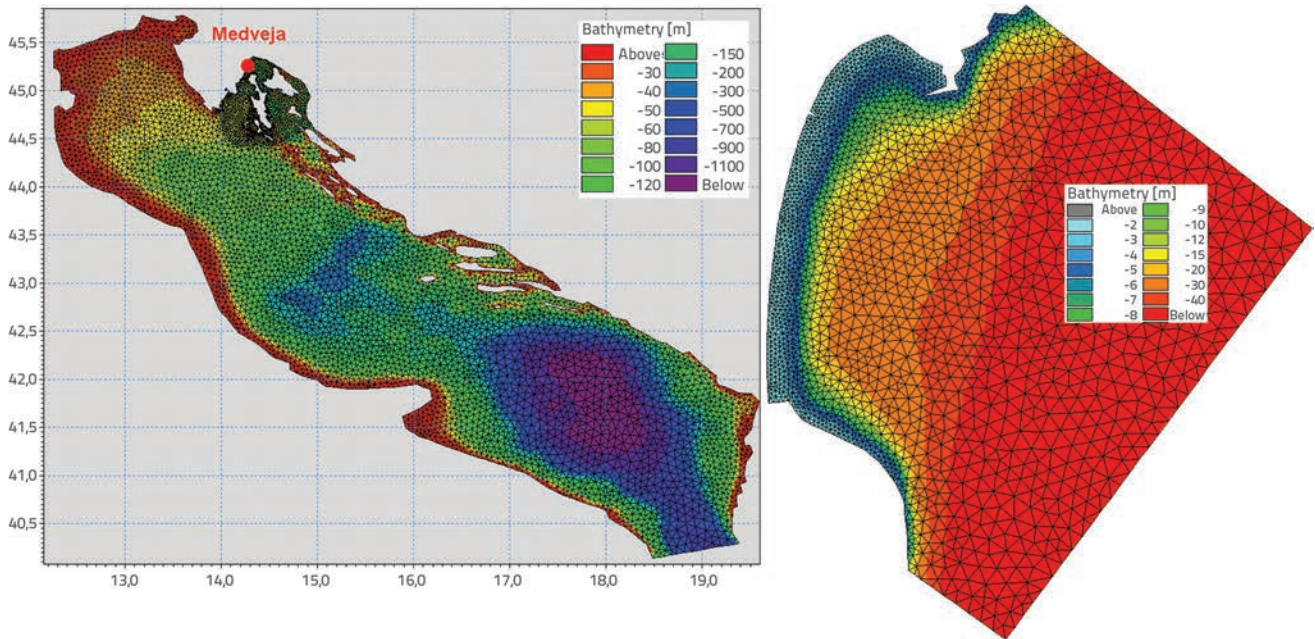

Figure 7. Spatial discretisation of model spatial domain with unstructured finite volume grid on bathymetric background (left – regional model; right – local model)
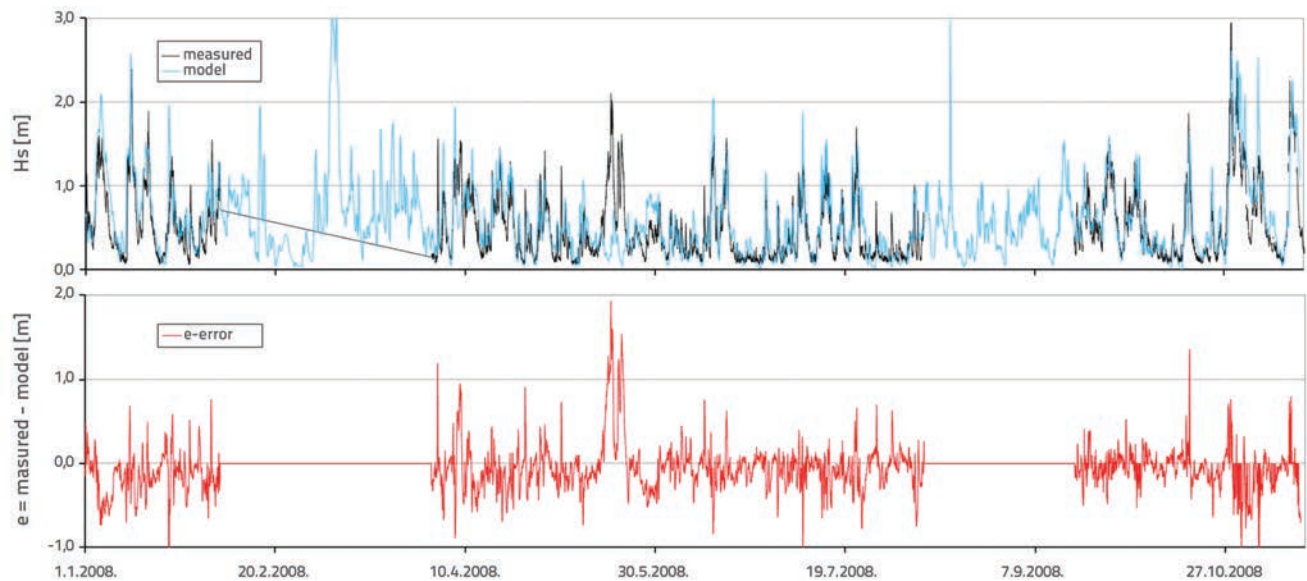

Figure 8. Comparison of measured and modelled time series of significant wave heights H_s at wave measuring station positions (above), and histogram error (e = wavegraph – model) model values H_s for numerical simulation conducted in 2008
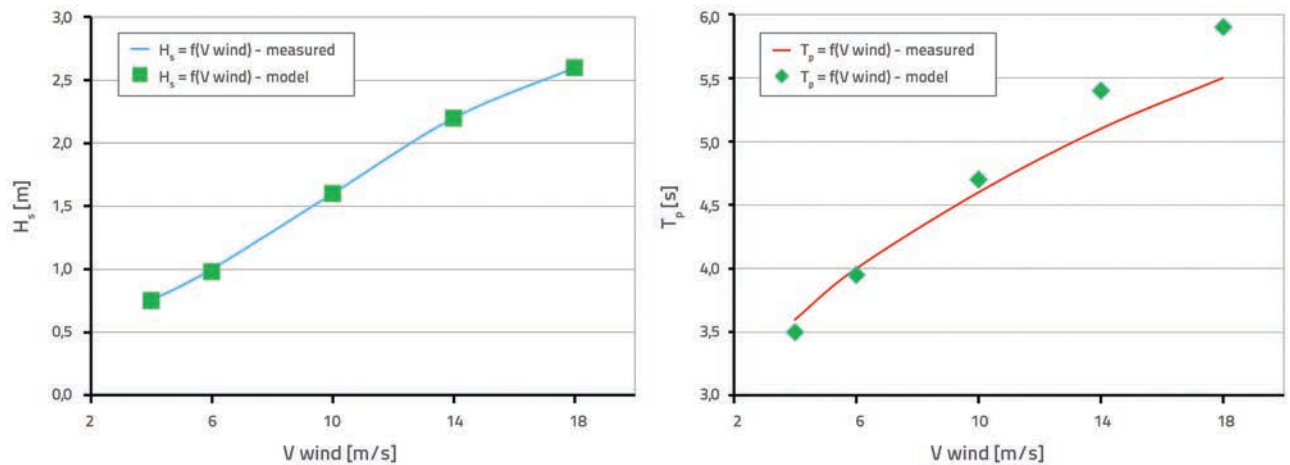
Figure 9. Relationship of measured and modelled significant wave heights H_s and peak period T_p against measured wind speed V_{wind} under action of wind from SSE direction in the course of 12 hours [37] (Petar Drapšan breakwater at Rijeka Harbour)
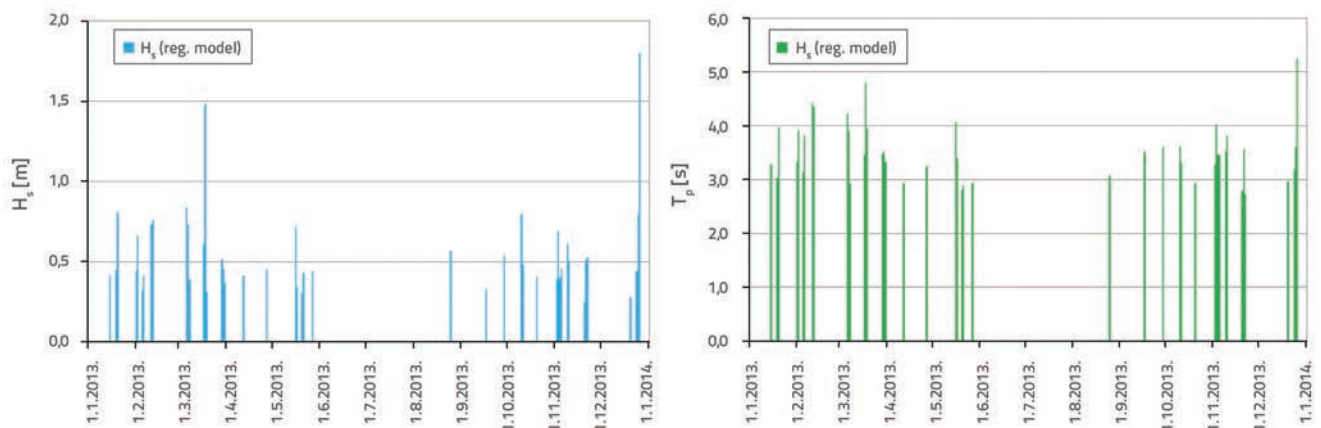

Figure 10. Wave performance according to adopted criteria for relevant situation ($H_s \geq 0.2$ m ; $T_p \geq 2.7$; incidental direction range 112^0 - 180^0)

Petar Drapšin in Rijeka Harbour (Figure 9). Figure 9 shows the relationship between the measured significant wave heights H_s and the peak period T_p against the measured wind speed V_{wind} for wind activity from the SSE direction with the duration of 12 hours [37]. Figure 9 also shows results of numerical simulation for the same site for stationary and homogenous winds of 4, 6, 10, 14, and 18 m/s.

Figure 10 shows wave performance according to the previously adopted criteria for relevant situations ($H_s \geq 0.2$ m ; $T_p \geq 2.7$; incidental direction range 112^0 - 180^0), for a deep-water point at the entrance to Medveja Bay (see Figure 5). A total of 42 locations were recognized (Table 3). The start point of each situation, its duration, the corresponding average significant wave height and peak period, as well as the maximum significant wave height, are listed in Table 3. It should be noted that, over the course of the simulation period, the largest wave at the entrance to Medveja Bay was registered on 11/11/2013 during the Bora wind. As the analysed profile did not reveal wave action from that incidental direction, such a situation is not essential

for the morphological profile development, and was not taken into consideration (documented below in this Section).

It can be seen from Figure 10 and the data presented in Table 3 that there was no stronger wave activity in the adopted range of incidental directions (112.5^0-180^0) during the analysed period from 17/03/2013 to 25/12/2013. In other words, a mild wave climate predominated over the nine months before the detailed bathymetry survey in Medveja Bay (Figure 5). Consequently, the morphodynamic beach analysis was further conducted in intensive storm conditions in 2013 (Table 3, Situation 42; 25/12/2013 to 26/12/2013, after the recording of 23/12/2013).

Figure 11 shows the fields of significant wave heights due to a strong Sirocco wind registered on 18/03/2013 at 13:00 (regional and local model), as well as the field of significant wave heights due to Bora storm (11/11/2013 10:00 ; local model). It can be seen in Figure 9 that the wave activity is generated by Sirocco wind in dominant storms covered by morphological presentation of the analysed longitudinal beach profile. Thus the application

Table 3. Start point of each situation, its duration, corresponding average significant wave height and peak period, as well as maximum significant wave height during each situation for deep-water points in front of Medveja Bay (results from regional model)

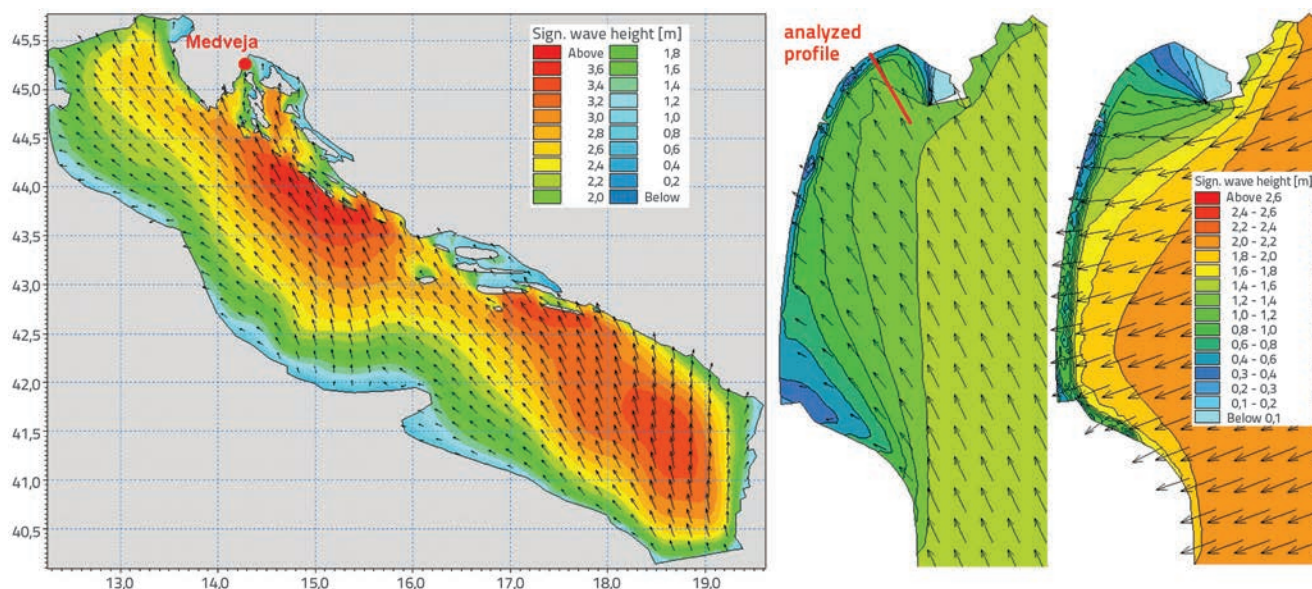|	situation onset (dd.mm.yyyy., hour)	duration [h]	H_{S-AV} [m]	T_{P-AV} [s]	H_{MAX} [m]		situation onset (dd.mm.yyyy., hour)	duration [h]	H_{S-AV} [m]	T_{P-AV} [s]	H_{MAX} [m]
		Deep water conditions						Deep water conditions			
1	15.1.2013., 10:00	12	0.26	3.1	0.32	22	16.5.2013., 2:00	36	0.31	3.4	0.55
2	19.1.2013., 21:40	3	0.33	2.9	0.33	23	17.5.2013., 16:40	3	0.17	3.0	0.17
3	20.1.2013., 2:00	18	0.49	3.6	0.54	24	20.5.2013., 22:00	3	0.21	2.8	0.21
4	24.1.2013., 20:20	3	0.22	3.1	0.22	25	21.5.2013., 13:40	3	0.29	2.8	0.29
5	1.2.2013., 0:00	15	0.45	3.6	0.52	26	23.5.2013., 15:40	3	0.32	2.8	0.32
6	4.2.2013., 15:40	3	0.29	3.1	0.29	27	27.5.2013., 9:20	3	0.33	2.8	0.33
7	5.2.2013., 21:40	3	0.24	3.0	0.24	28	26.6.2013., 13:40	3	0.37	2.8	0.37
8	6.2.2013., 6:00	6	0.27	3.4	0.32	29	25.8.2013., 14:00	3	0.41	3.0	0.41
9	11.2.2013., 16:00	12	0.46	4.0	0.58	30	2.9.2013., 3:40	3	0.29	2.9	0.29
10	19.2.2013., 12:00	3	0.39	3.4	0.39	31	17.9.2013., 4:00	6	0.42	3.2	0.23
11	6.3.2013., 7:00	36	0.47	3.5	0.65	32	29.9.2013., 9:00	9	0.39	3.2	0.40
12	11.3.2013., 4:40	3	0.33	3.0	0.33	33	10.10.2013., 14:00	21	0.42	3.2	0.60
13	17.3.2013., 15:00	39	0.59	3.8	1.14	34	20.10.2013., 15:00	6	0.31	2.9	0.32
14	25.3.2013., 20:00	3	0.30	3.3	0.30	35	2.11.2013., 12:00	42	0.31	3.3	0.54
15	29.3.2013., 6:00	6	0.34	3.3	0.40	36	7.11.2013., 21:40	3	0.28	2.9	0.28
16	30.3.2013., 10:40	3	0.30	3.1	0.30	37	9.11.2013., 7:00	33	0.35	3.3	0.48
17	31.3.2013., 1:00	3	0.30	3.3	0.30	38	17.11.2013., 14:40	3	0.31	2.9	0.31
18	8.4.2013., 9:20	3	0.30	2.9	0.30	39	21.11.2013., 15:00	6	0.38	3.4	0.40
19	12.4.2013., 15:00	3	0.32	2.9	0.32	40	10.12.2013., 23:40	3	0.29	2.8	0.29
20	22.4.2013., 16:40	3	0.33	2.9	0.33	41	20.12.2013., 13:00	3	0.20	2.9	0.20
21	27.4.2013., 19:00	3	0.24	3.0	0.24	42	25.12.2013., 9:00	36	0.78	4.1	1.39

Figure 11. Fields of significant wave heights in case of a strong Sirocco wind (situation 13 – 18/03/2013 13:00) obtained with regional (left) and local (centre) wave generation model, and the wave deformation field of significant wave heights due to Bora wind (11/11/2013 10:00) obtained from local model (right)

Goran Lončar, Dalibor Carević, Damir Bekić, Maria Babić, Nina Grbić, Vjera Pranjić

Table 4. Amplitudes and phases of tidal constituents used in the synthesis of sea level at Bakar location [38]

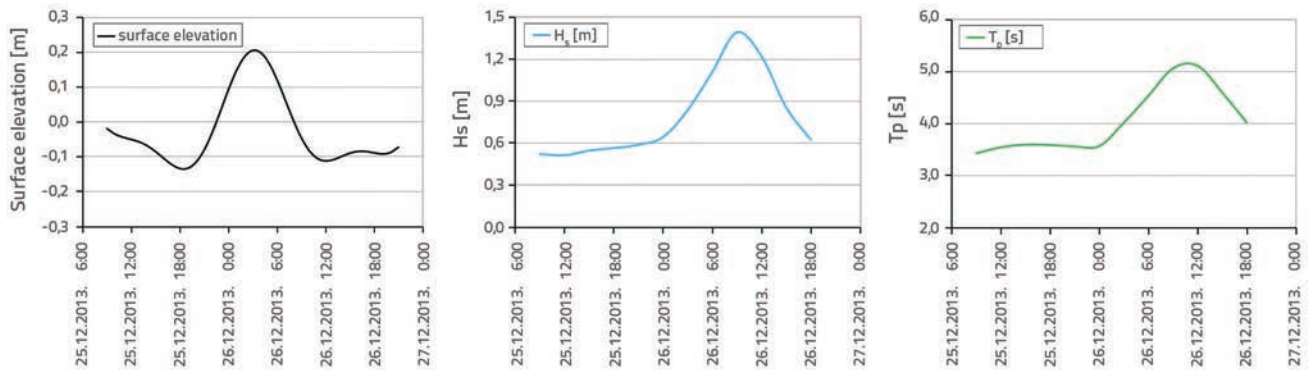| O1		P1		K1		N2		M2		S2		K2	
amp	faza	amp	faza	amp	faza	amp	faza	amp	faza	amp	faza	amp	faza
[cm]	[°]	[cm]	[°]	[cm]	[°]	[cm]	[°]	[cm]	[°]	[cm]	[°]	[cm]	[°]
4.41	53.1	5	65.4	14.06	67.4	1.96	252	10.32	250.1	5.75	250.4	1.71	235.4

Figure 12. Boundary conditions of Xbeach-G model (calm sea level H_s, T_p) defined with three hour resolution

of the one-dimensional morphodynamic model (XBeach-G) along the analysed beach profile is considered justified.

The modelled initial beach profile (23/12/2013) is identical to the measured profile (Figure 5). In comparison to the numerical simulation for d_{50}, the value of 14.5 mm was adopted according to laboratory analysis results of the sample taken at beach front (Figure 5) The dynamics of the sea surface *level is taken* into account with seven basic tidal signal constituents [38] (Table 4, Figure 12). It is important to note that boundary conditions of the XBeach-G model (H_s, T_p, sea surface elevation, figure 11) are defined with the three-hour resolution.

Figure 13 shows the measured beach profile registered on 23/12/2013, calculated profile in the middle (26/12/2013) and at the end of the simulated period (26/12/2013 18:00), and the profile obtained based on empirical formulae [10,11].
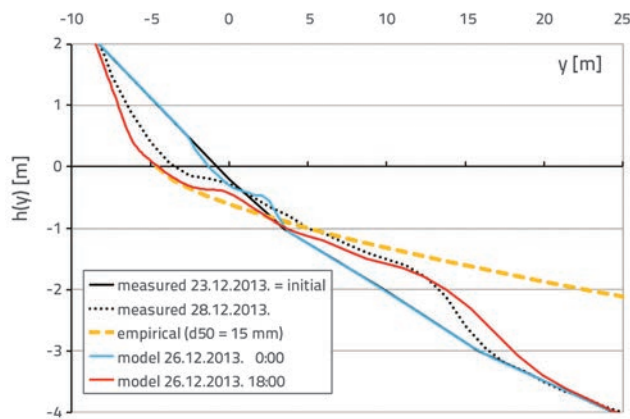

Figure 13. Beach profiles measured on 23/12/2013 (initial) and 28/12/2013, modelled profiles in the middle (26/12/2013 0:00) and the end (26/12/2013 18:00) of the simulation period (situation 42 from Table 3), and equilibrium profile according to empirical terms [10, 11]

The total eroded area obtained by numerical morphodynamic calculation amounts to 6.5 m² (Figure 13). According to the empirical formula (1) and the diagram of erosion shown in Figure 4, and based on the adopted values of H_s = 1.08 m ; T_p = 4.66 s (average values for the period ranging from 26/12/2013 3:00 to 26/12/2013, 15:00, see Figure 12); d_{50} = 14.5 mm; $\rho_{\check{s}}$ = 2600 kg/m³; ρ_M = 1028 kg/m³; N = 9734; P = 25 %; tan α = 0.22 (from -2 to +2 m), the values of the eroded area amount to 45.6 m² (empirical formula (1)) and 6.2 m² (application of the diagram shown in Figure 3). The eroded area of the profile measured on 28/12/2013, as related to the profile measured on 23/12/2013, amounts to 4.5 m².

6. Conclusion

A morphodynamic analysis of the cross-sectional profile of gravel beaches under the action of wind waves was conducted. In order to include a range of characteristic environmental conditions in the analysis, the following parameters were varied: initial beach slope (from 1:10 to 1:4), steepness of deep-water waves (from 1:10 to 1:25), and gravel grain diameter (from 10 to 30 mm).

The XBeach-G numerical model was used in the research, as well as an empirical formula for calculating the dynamically-stable beach profiles, and estimating the eroded area along the profile. Diagrams generated on the basis of numerical model results enable a simple estimate of the anticipated amount of eroded beach material in correlation with the prevailing wave conditions, and also initial selection of beach slope, and determination of the filling material grading.

Boundary conditions obtained by numerical simulation of wave generation and wave deformation on a wide spatial scale were used for further analysis of morphodynamics of the real profile of the Medveja gravel beach.

These results enabled presentation of practical application of the diagram for estimating erosion of the real beach profile under real wave conditions, and comparison with results obtained by empirical formulae. It is important to note that the calculations were performed for moderate waves that prevailed during the simulation period, while the greatest attention in the design of gravel beaches is paid to the beach deformation under the extreme sea wave action.

Average values of significant wave heights and peak wave periods were used for direct application of the erosion diagram. These values were analysed for extreme situations, and the estimate obtained for the eroded profile area (6.2 m²) is close to the detailed numerical calculation results (6.5 m²) and measurement results (4.5 m²). The empirical form applied for estimating the eroded area resulted in multiple exceedances of measured and modelled values, and is not recommended for application. The obtained results show that practical application of the presented diagrams may be useful in different, mostly early, phases of beach project design.

It should be noted that the presented conclusions on the stability of the analysed cross-sectional profile of Medveja Beach cannot be applied globally (for the entire beach). For the extension of the present research, it would be necessary to use a more complex numerical model (2D or 3D) and to analyse inhomogeneous characteristics of beach material.

REFERENCES

[1]   Austin, M.J., Masselink, G.: Observations of morphological change and sediment transport on asteep gravel beach, *Marine Geology*, 229 (2006) 1-2, pp. 59-77.

[2]   Carter, R.W.G., Orford, J.D.: The morphodynamics of coarse clastic beaches and barriers: a short term and long term perspective, *J. Coast. Res.* Special issue, 15 (1993), pp.158-179.

[3]   McKay, P.J., Terich, T.A.: Gravel barrier morphology: Olympic National Park,Washington State, USA, *J. Coast. Res.*, 8 (1992) 4, pp. 813-829.

[4]   Forbes, D.L., Orford, J.D., Carter, R.W.G., Shaw, J., Jennings, S.C.: Morphodynamic evolution, self-organisation and instability of coarse clastic barriers on paraglacial coasts, *Mar. Geol,* 126 (1995) 1-4, pp. 63-85.

[5]   Ojeda, E., Guillen, J.: Shoreline dynamics and beach rotation of artificial embayed beaches, *Mar. Geol,* 253 (2008) 1-2, pp. 51-62.

[6]   Curtiss, G. M., Osborne, P. D., Horner-Devine, A. R.: Seasonal patterns of coarse sediment transport on a mixed sand and gravel beach due to vessel wakes, wind waves, and tidal currents, *Mar. Geol*, 259 (2009) 1-4, pp. 73-85.

[7]   Poate, T., Masselink, G., Davidson, M., McCall, R., Russell, P., Turner, I.: High frequency in-situ field measurements of morphological response on a fine gravel beach during energetic wave conditions, *Mar. Geol*, 342 (2013), pp. 1-13, http://dx.doi.org/10.1016/j.margeo.2013.05.009

[8]   Orford, J.D.: A proposed mechanismfor stormbeach sedimentation, *Earth Surf. Proc. Land*, 2 (1977) 4, pp. 381-400.

[9]   Almeida, L., Masselink, G., Russell, P., Davidson, M., Poate, T., McCall, R., Blenkinsopp, C., Turner, I.: Observations of the swash zone on a gravel beach during a storm using a laser-scanner, *Journal of Coastal Research*, Special Issue No. 65, Proceedings 12th International Coastal Symposium, Plymouth, (2013), pp. 636-641.

[10] USACE: *Coastal Engineering manual*, Part III, EM 1110-2-1100, 2008.

[11] Dean, R.G.: Coastal Sediment Processes: Toward Engineering Solutions, *Proc. Coastal Sediments*, ASCE, New Orleans, pp.1-24, 1987.

[12] Van der Meer, J. W.: Stability of breakwater armour layers - design formulae, *Coastal Engineering*, Elsevier Science Publishers B.V, Amsterdam, pp. 234, 1987.

[13] Bradbury, A.P.: Predicting breaching of shingle barrier beaches - recent advances to aid beach management, *Papers and Proceedings 35th MAFF (DEFRA) Conference of River and Coastal Engineers*, Keele, pp. 05.3.1-05.3.13, 2000.

[14] Obhrai, C., Powell, K., Bradbury, A.: A laboratory study of overtopping and breaching of shingle barrier beaches, *Proceedings of 31st International Conference on Coastal Engineering*, Hamburg, pp. 1497-1508, 2008.

[15] Bradbury, A., Cope, S., Prouty, D.: Predicting the response of shingle barrier beaches under extreme wave and water level conditions in Southern England, *Proc. 5th International Coastal Dynamics Conference*, Barcelona, pp. 1-14, 2005.

[16] Cope, S.: Predicting overwashing and breaching of coarse - clastic barrier beaches and spits - application to Medmerry, West Sussex, Southern England, *Proc. 5th International Coastal Dynamics Conference*, Barcelona, pp. 1-14, 2005.

[17] Roelvink, J.A., Reniers, A., van Dongeren, A.R., van Thiel de Vries, J.S.M., McCall, R., Lescinski, J.: Modeling storm impacts on beaches, dunes and barrier islands, *Coastal Engineering*, 56 (2009) 11-12, pp. 1133-1152.

[18] Tuan, T.Q., Verhagen, H.J., Visser, P., Stive, M.J.F.: Numerical modelling of wave overwash on low-crested sand barriers, *30th Coastal Engineering Conference*. World Scientific, San Diego. 2006.

[19] Jamal, M.H., Simmonds, D., Magar, V.: Modelling gravel beach dynamics with XBeach, *Coast. Eng*, 89 (2014), pp. 20-29.

[20] Pedrozo-Acuna, A., Simmonds, D., Otta, A.K., Chadwick, A.J.: On the cross-shore profile change of gravel beaches, *Coast. Eng.*, 53 (2006) 4, pp. 335-347.

[21] Williams, J., de Alegría-Arzaburu, A.R., McCall, R.T., van Dongeren, A.: Modelling gravel barrier profile response to combinedwaves and tides using XBeach: laboratory and field results, *Coast. Eng.*, 63 (2012), pp. 62-80, http://dx.doi.org/10.1016/j.coastaleng.2011.12.010

[22] McCall, R., Masselink, G., Roelvink, J., Russell, P., Davidson, M., Poate, T.: Modeling overwash and infiltration on gravel barriers, *Proceedings of the 33rd International Conference on Coastal Engineering*, Santander, pp. 1-48, 2012.

[23] McCall, R.T., Masselink, G., Poate, T.G., Roelvink, J.A., Almeida, L.P., Davidsona, M., Russell, P.E.: Modelling storm hydrodynamics on gravel beaches with XBeach-G, *Coast. Eng.*, 91 (2014), pp. 231-250, http://dx.doi.org/10.1016/j.coastaleng.2014.06.007

[24] MacCormack, R.W.: The effect of viscosity in hypervelocity impact cratering, *AIAA Hyper Velocity Impact Conference*, Cincinnati, pp. 69-354, 1969., http://dx.doi.org/10.2514/6.1969-354

[25] Smit, P., Stelling, G., Roelvink, J., Van Thiel de Vries, J., McCall, R., Van Dongeren, A., Zwinkels, C., Jacobs, R.: XBeach: non-hydrostatic model: validation, verification and model description, Delft University of Technology, 2010.

[26] Stelling, G.S., Duinmeijer, S.P.A.: A staggered conservative scheme for every Froude number in rapidly varied shallow water flows. Int. J. Numer. Methods Fluids, 43 (2003) 12, pp. 1329-1354, http://dx.doi.org/10.1002/fld.537

[27] Smagorinsky, J.: General circulation experiments with the primitive equations. *Mon. Weather Rev.*, 91 (1963) 3, pp. 99-164, http://dx.doi.org/10.1175/1520-0493(1963)091<0099:GCEWTP>2.3.CO;2

[28] Stelling, G.S., Zijlema, M.: An accurate and efficient finite-difference algorithm for non-hydrostatic free-surface flow with application to wave propagation. Int. J. Numer. Methods Fluids, 43 (2003), pp. 1-23, http://dx.doi.org/10.1002/fld.595

[29] Halford, K.: Simulation and interpretation of borehole flowmeter results under laminar and turbulent flow conditions. Proceedings of the Seventh International Symposium on Logging for Minerals and Geotechnical Applications, Golden, Colorado. The Minerals and Geotechnical Logging Society, pp. 157-168, 2000.

[30] Packwood, A.: The influence of beach porosity on wave uprush and backwash. Coast. Eng., 7 (1983) 1, pp. 29-40, http://dx.doi.org/10.1016/0378-3839(83)90025-X

[31] Goda, Y.: *Random Seas and Design of Maritime Structures*, Advanced series on ocean engineering, Worl Scientific Ed., New Jersey, 2000.

[32] Horn, D.P.: Beach groundwater dynamics, Geomorphology, 48 (2002), pp. 121-146, http://dx.doi.org/10.1016/S0169-555X(02)00178-2

[33] Komen, G., J., Cavaleri, M., Donelan, K., Hasselman, S., Hasselman, K., Janssen, P.A.E.M.: *Modelling of dynamic of ocean surface waves*, Cambridge university press, Cambridge, pp. 532, 1994.

[34] Hercbach, H., Janssen, P.A.E.: *Improvement of the short-fetch behaviour in the Wave Ocean Model (WAM)*, J. Atmos and Ocean Tech., 16 (1999), pp. 884-892, http://dx.doi.org/10.1175/1520-0426(1999)016<0884:IOTSFB>2.0.CO;2

[35] Građevinski institut: "Hidraulička analiza valova i nasipnih konstrukcija sjeverne obale brodogradilišta 3. Maj u Rijeci", Građevinski institut, 1991. (in Croatian)

[36] Brzović, N., Strelec-Mahović, N.: *Cyclonic activity and severe jugo in the Adriatic*, Physics and Chemistry of the Earth *(B)*, 24 (1999), pp. 653-657, http://dx.doi.org/10.1016/S1464-1909(99)00061-1

[37] Ivatek-Sahdan, S., Tudor, M.: *Use of high-resolution dynamical adaptation in operational suite and research impact studies*, Meteorol. Z., 13 (2004), pp. 99-108, http://dx.doi.org/10.1127/0941-2948/2004/0013-0099

[38] Janeković, I., Kuzmić, M.: Numerical simulation of the Adriatic Sea principal tidal constituents, Ann. Geophys., 23 (2005), pp. 3207-3218.